Multiple Interactions in DIS

Henri Kowalski
Deutsches Elektronen Synchrotron DESY, 22603 Hamburg

Abstract
The abundance of diffractive reactions observed at HERA indicates the presence of multiple interactions in DIS. These interactions are analysed, first in a qualitative way, in terms of QCD Feynman diagrams. Then a quantitative evaluation of diffractive and multiple interaction is performed with the help of the AGK cutting rules applied within an Impact Parameter Dipole Saturation Model. The cross-sections for multiple and diffractive interactions are found to be of the same order of magnitude and to exhibit a similar Q^2 dependence.

1 Introduction

One of the most important observations of HERA experiments is the rapid rise of the structure function F_2 with decreasing x indicating the presence of abundant gluon radiation processes [1]. The observation of a substantial diffractive component in DIS processes, which is also quickly rising with decreasing x, is equally important. The diffractive contribution at HERA is of a leading-twist type, i.e. the fraction of diffractive events remains constant or decreases only logarithmically with increasing Q^2. The presence of a substantial diffractive component suggests that, in addition to the usual partonic single ladder contribution, also multi-ladder processes should be present.

In this talk I will first discuss the general role of multi-ladder contributions in DIS scattering, called for historical reasons multi-Pomeron processes. The concept of a Pomeron is very useful in the discussion of high energy scattering processes since it relates, by the AGK cutting rules [2], seemingly different reactions like inclusive, diffractive and multiple scattering. I will present a numerical estimate of the magnitude of diffractive and of multi-Pomeron contributions, using AGK cutting rules within a dipole model which has been shown to provide a good description of HERA DIS data [3].

2 General Analysis

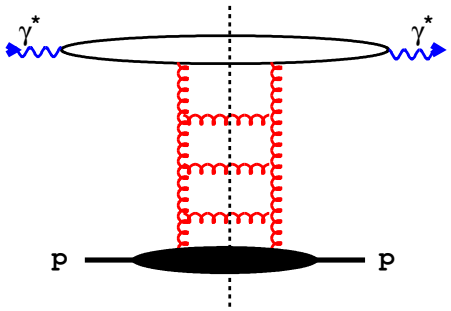

Fig. 1: The single gluon-ladder contribution to the total $\gamma^* p$ cross section. The blob at the lower end of the diagrams contains the physics below the scale Q_0^2 which seperates hard from soft physics, whereas the blob at the upper end contains hard physics that can be described by pQCD. The dashed line denotes the cut.

Let us first recall that the main properties of HERA interactions can be related to the properties of the elastic amplitude, $A_{\gamma^* p \to \gamma^* p}$, which, by the optical theorem, is directly related to the total $\gamma^* p$ cross-section:

$$\sigma_{\gamma^* p} = \frac{1}{W^2} Im\, A_{\gamma^* p \to \gamma^* p}(W^2, t=0). \tag{1}$$

Here W denotes the $\gamma^* p$ CMS energy and t the 4-momentum transfer of the elastically scattered proton. At not too small Q^2, the total cross section is dominated by the single ladder exchange shown in Fig. 1; the ladder structure also illustrates the linear DGLAP evolution equations that are used to describe the F_2 data. In the region of small x, gluonic ladders are expected to dominate over quark ladders. The cut lines in Fig. 1 mark the final states produced in a DIS event: a cut parton (gluon) hadronizes and leads to jets or particles seen in the detector. It is generally expected that partons produced from a single chain are unlikely to generate large rapidity gaps between them, since large gaps are exponentially suppressed as a function of the gap size. Therefore, in the single ladder contribution of Fig. 1, diffractive final states only reside inside the blob at the lower end, i.e. lie below the initial scale Q_0^2.

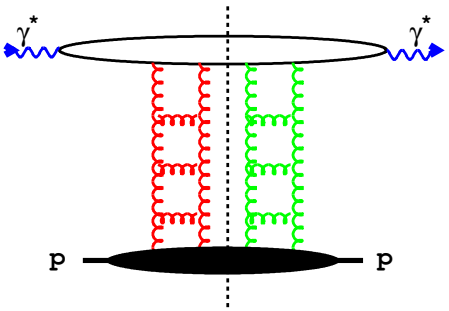

Fig. 2: The double-gluon ladder contribution to the inclusive diffractive $\gamma^* p$ cross section

The properties of diffractive reactions at HERA, however, give clear indications that significant contributions from multi-ladder exchanges should be present: not all diffractive final states are soft, in particular the diffractive production of jets and charm was observed [4, 5]. In addition, the inclusive diffractive cross-section is rising as quickly as the total cross-section with increasing W [6] and the exclusive diffractive production of J/Ψ and Υ vector meson exhibits a rise with energy which is about twice as fast [7]. In short, the Pomeron exchanged in inclusive diffractive DIS is harder than the hadronic soft Pomeron and therefore, one should expect that the majority of the observed diffractive final states cannot be absorbed into the blob of soft physics of Fig. 1. Instead, double ladder exchange, Fig. 2, provides a potential source for these harder diffractive states: the cut blob at the upper end may contain $q\bar{q}$ and $q\bar{q}g$ states which hadronize into harder jets or particles. Further evidence for the presence of multi-ladder contribution comes from saturation models which have been shown to successfully describe HERA F_2 data in the transition region at low Q^2 and small x: these models are explicitly built on the idea of summing over multiple exchanges of single ladders (or gluon densities).

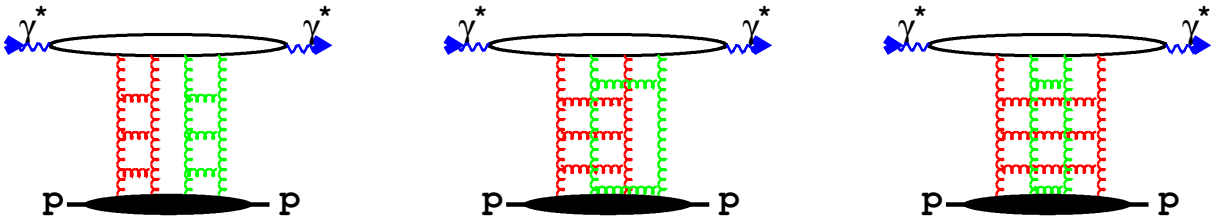

Fig. 3: The double-gluon ladder contribution to the elastic $\gamma^* p$ amplitude

Let us analyse the content of a double ladder exchange contribution (for a more detailed analysis see Ref. [8]). It is easiest to begin with the elastic $\gamma^* p$ scattering amplitude, Fig. 3: from a t-channel point of view, the two gluon ladders form a four gluon intermediate state which has to be symmetric under permutations of the gluon lines (Bose symmetry). Therefore, on the amplitude level one cannot distinguish between different diagrams of Fig. 3. Invoking now the optical theorem, (1), different contributions to the total cross section correspond to different cuts through the two-ladder diagrams: they

are shown in Fig. 4, ordered w.r.t. the density of cut gluons. In Fig. 4a, the cut runs between the two ladders: on the both sides of the cut there is a color singlet ladder, and we expect a rapidity gap between the upper blob (containing, for example, a diffractive $q\bar{q}$ final state) and the proton remnants inside the lower blob. Similarly, the diagram of Fig. 4b describes a single cut ladder with a final state similar to the one ladder contribution in Fig. 1; this contribution simply represents a correction to the one ladder contribution. Finally, the diagram of Fig. 4c belongs to final states with double density of cut partons. As outlined in [9], the correct counting of statistic factors and combinatorics leads to the result that the contributions shown in Fig. 4 a - c are identical, up to the overall counting factors $1 : -4 : 2$.

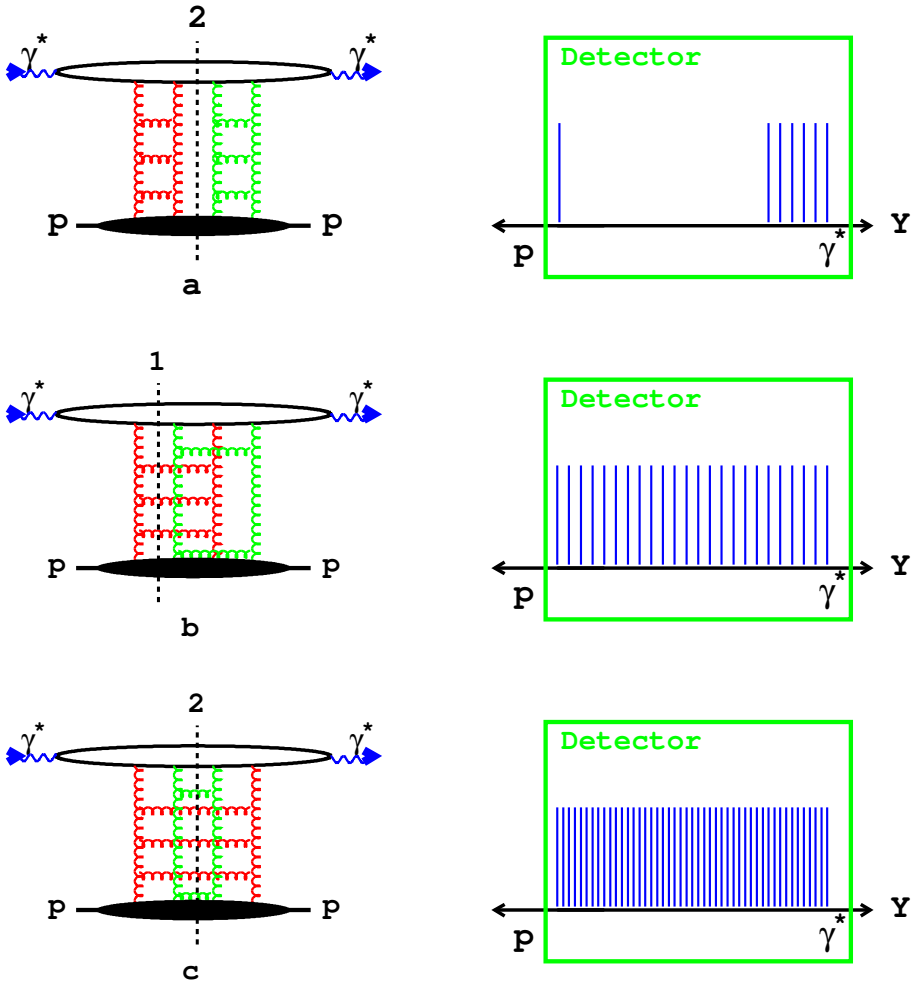

Fig. 4: Three examples of 2-ladder contributions (lhs), with the corresponding, schematical, detector signatures (rhs). *Top row*: the diagram (a) with the cut positions (2) describes diffractive scattering. *Middle row*: the diagram (b) with the cut position (1) describes inclusive final states with single densityof cut partons. *Bottom row*: the diagram (c) with the cut position (2) describes inclusive final states with increased multiplicity.

Experimentally it is easy to differentiate between diffractive and *single* or *multiple* inclusive final states since diffractive states exhibit large rapidity gaps. The *multiple* inclusive final states should also be distinct from the *single* inclusive ones since, at least naively, we would expect that in the *multiple* case the particle multiplicity should be considerably higher. At low x, however, the relation between the number of virtual states excited in the interaction (as measured by F_2) and the final particle multiplicity cannot be straight-forward since the growth of F_2 with decreasing x is faster than the multiplicity increase. This may indicate that the hadronization mechanism may be different from the string picture commonly used in the hadronization procedure of single chain parton showers. The influence of multiple scattering on

the particle multiplicity of the final states should also be damped by the energy conservation. The cut through several Pomerons leads clearly to more gluons produced in the final state, but the available energy to produce particles in the hadronization phase remains the same. A detailed Monte Carlo program is therefore necessary to evaluate this effect.

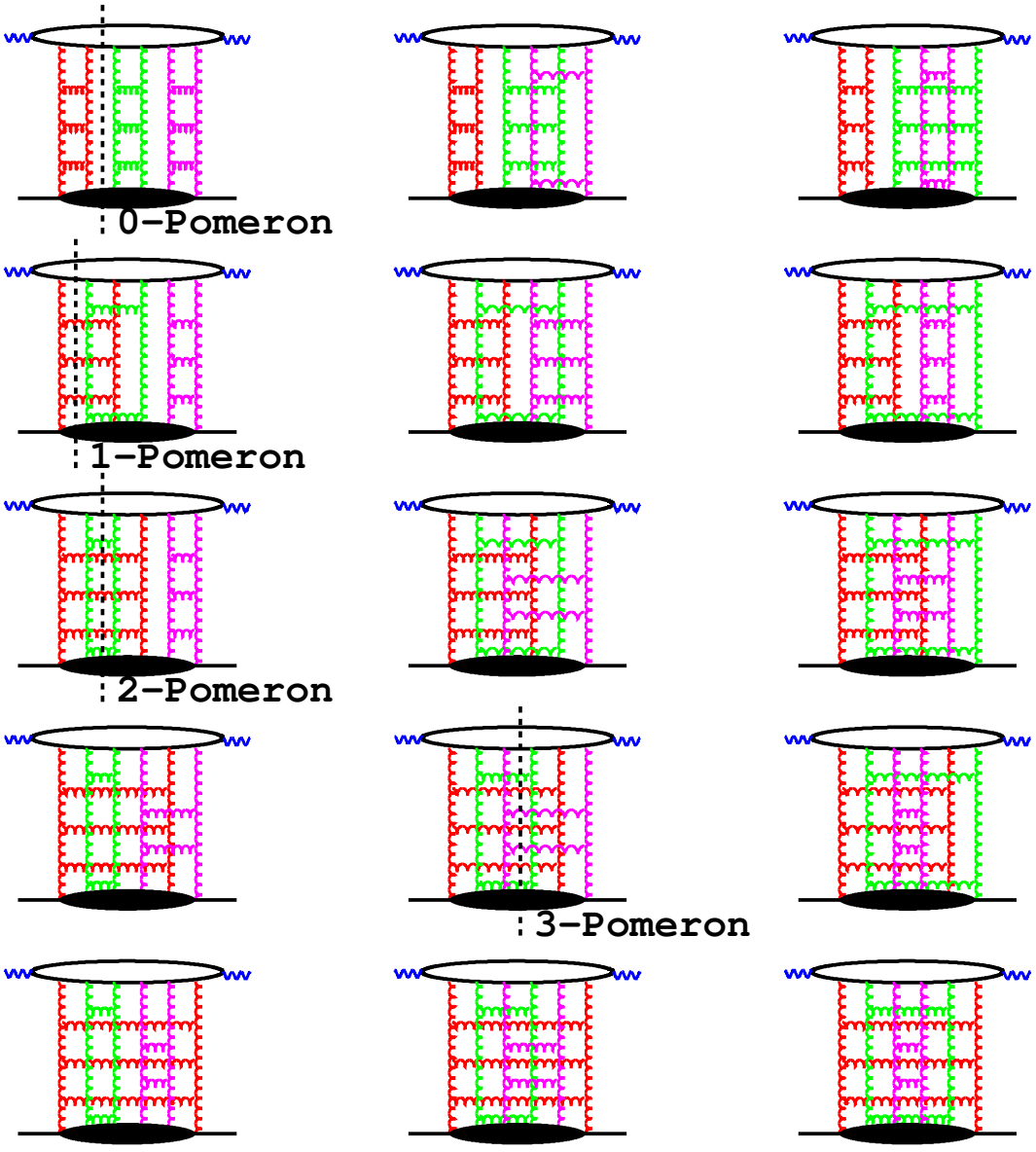

Fig. 5: 3-Pomeron contributions to the elastic $\gamma^* p$ amplitude. All 15 possible diagrams are shown with some examples of Pomeron cuts.

The number of diagrams contributing to the reaction amplitude increases very quickly with the number of Pomerons. For the 3-Pomeron amplitude the gluons can be paired in 15 possible ways, shown in Fig. 5 with the examples of 0-Pomeron, 1-Pomeron, 2-Pomeron and 3-Pomeron cuts. For m-Pomerons the number of possible gluon pairs and also diagrams is:

$$(2m-1)(2m-3)(2m-5)....=(2m-1)!/(2^{m-1}(m-1)!).$$

Assuming that all the diagrams for a given multi-Pomeron exchange amplitude contribute in the same way, the above analysis suggests that the probability for different cuts to contribute should be given

by the combinatorial factors. This is the content of the AGK rules which were obtained from the analysis of field theoretical diagrams well before QCD was established [2] and which relate the cross-section, σ_k, for observing a final state with k-cut Pomerons with the amplitudes for exchange of m Pomerons, $F^{(m)}$:

$$\sigma_k = \sum_{m=k}^{\infty} (-1)^{m-k}\, 2^m\, \frac{m!}{k!(m-k)!} F^{(m)}. \tag{2}$$

The same result is also obtained from a detailed analysis of the Feynman diagram contributions in QCD with the oversimplified assumption that only the symmetric part of the two-gluon couplings contributes [9].

3 Multiple Interactions in the Dipole Model

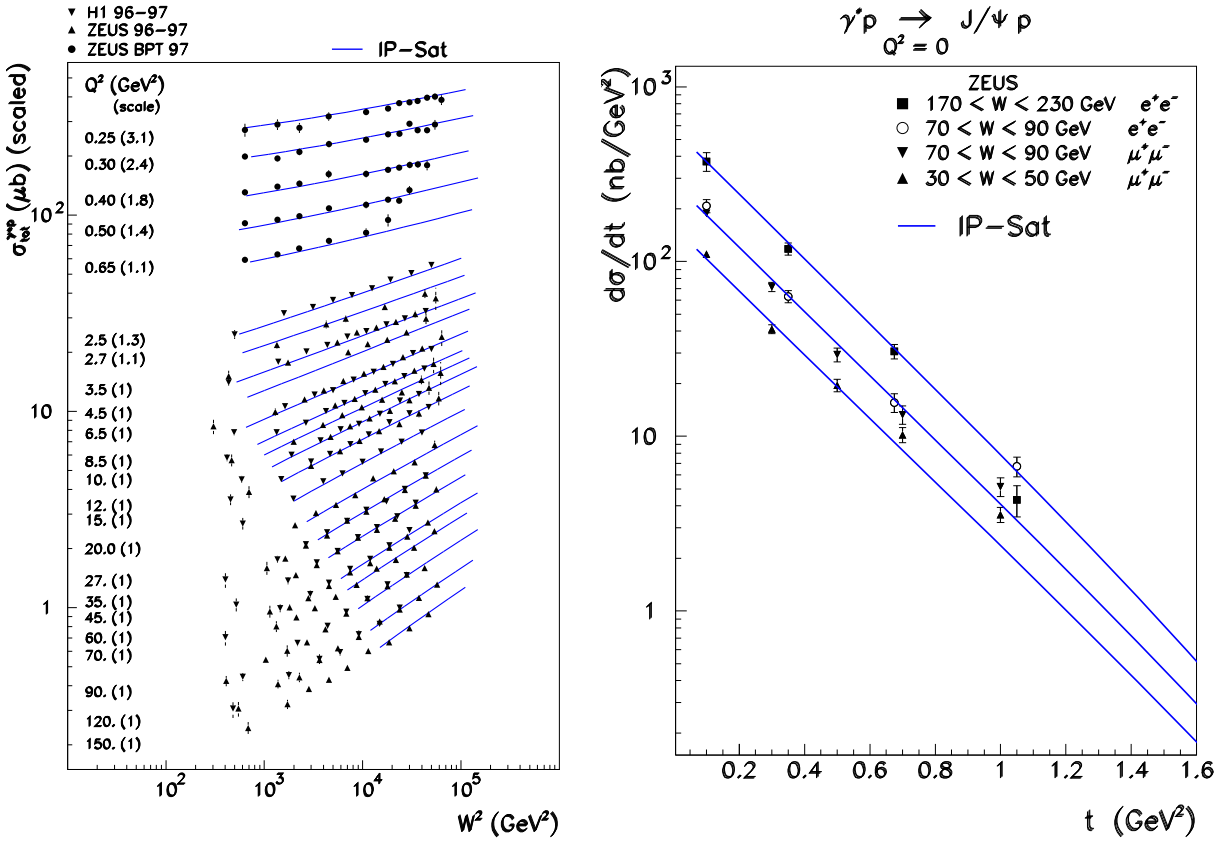

Fig. 6: LHS: The $\gamma^* p$ cross-section as a function of W^2. RHS: The differential cross section for exclusive diffractive J/Ψ production as a function of the four-momentum transfer t. The solid line shows a fit by the IP saturation model.

The properties of the multi-Pomeron amplitude and of the cut Pomeron cross-sections can be quantitatively studied in a dipole model. Let us first recall the main properties of the dipole picture, see Ref. [10, 11] and [3]. In the model the $\gamma^* p$ interaction proceeds in three stages: first the incoming vitual photon fluctuates into a quark-antiquark pair, then the $q\bar{q}$ pair elastically scatters on the proton, and finally the $q\bar{q}$ pair recombines to form a virtual photon. The total cross-section for $\gamma^* p$ scattering, or equivalently F_2, is obtained by averaging the dipole cross-sections with the photon wave functions, $\psi(r, z)$, and integrating over the impact parameter, b:

$$F_2 = \frac{Q^2}{4\pi^2 \alpha_{em}} \int d^2r \int \frac{dz}{4\pi} \psi^* \psi \int d^2b \frac{d\sigma_{qq}}{d^2b}\,. \tag{3}$$

Here $\psi^*\psi$ denotes the probability for a virtual photon to fluctuate into a $q\bar{q}$ pair, summed over all flavors and helicity states. The dipole cross-section is assumed to be a function of the opacity Ω:

$$\frac{d\sigma_{qq}}{d^2b} = 2\left(1 - \exp(-\frac{\Omega}{2})\right) . \tag{4}$$

At small-x the opacity Ω can be directly related to the gluon density, $xg(x,\mu^2)$, and the transverse profile of the proton, $T(b)$:

$$\Omega = \frac{\pi^2}{N_C} r^2 \, \alpha_s(\mu^2) \, xg(x,\mu^2) \, T(b) . \tag{5}$$

The parameters of the gluon density are determined from the fit to the total inclusive DIS cross-section, as shown in Fig. 6 [3]. The transverse profile was determined from the exclusive diffractive J/Ψ cross-sections shown in the same figure. The opacity function Ω determined in this way has predictive properties; it allows to describe other measured reactions, e.g. charm structure function or elastic diffractive J/Ψ production shown in Fig.7.

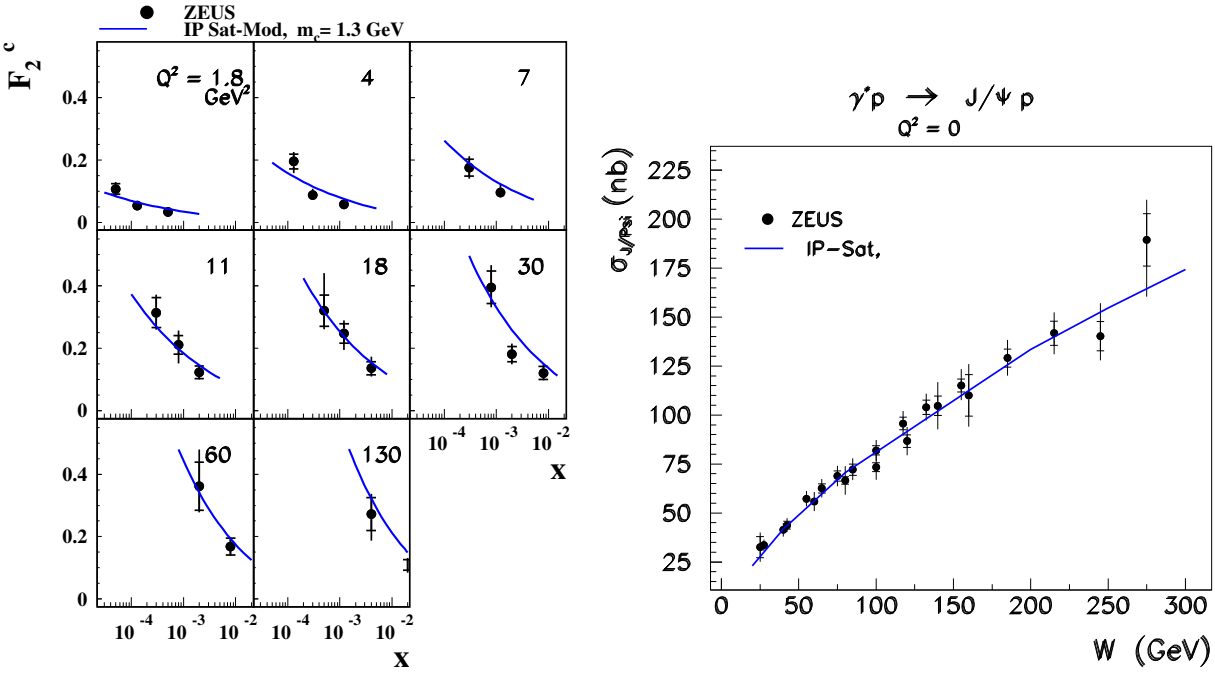

Fig. 7: LHS: Charm structure function, F_2^c. RHS: Total elastic J/Ψ cross-section. The solid line shows the reswult of the IP saturation model.

For a small value of Ω the dipole cross-section, Eq (4), is equal to Ω and therefore proportional to the gluon density. This allows to identify the opacity with the single Pomeron exchange amplitude of Fig. 1. The multi-Pomeron amplitude is determined from the expansion:

$$\frac{d\sigma_{qq}}{d^2b} = 2\left(1 - \exp(-\frac{\Omega}{2})\right) = 2\sum_{m=1}^{\infty}(-1)^{m-1}\left(\frac{\Omega}{2}\right)^m \frac{1}{m!} \tag{6}$$

as

$$F^{(m)} = \left(\frac{\Omega}{2}\right)^m \frac{1}{m!}, \tag{7}$$

since the dipole cross-section can be expressed as a sum of multi-Pomeron amplitudes [12] in the following way:

$$\frac{d\sigma_{qq}}{d^2b} = 2\sum_{m=1}^{\infty}(-1)^{m-1}\,F^{(m)}\,. \tag{8}$$

The cross-section for k cut Pomerons is then obtained from the AGK rules, eq. 2, and from the multi-Pomeron amplitude, Eq. (7), as:

$$\frac{d\sigma_k}{d^2b} = \sum_{m=k}^{\infty}(-1)^{m-k}\,2^m\,\frac{m!}{k!(m-k)!}\left(\frac{\Omega}{2}\right)^m\frac{1}{m!} = \frac{\Omega^k}{k!}\sum_{m=k}^{\infty}(-1)^{m-k}\,\frac{\Omega^{m-k}}{(m-k)!} \tag{9}$$

which leads to a simple expression:

$$\frac{d\sigma_k}{d^2b} = \frac{\Omega^k}{k!}\exp(-\Omega)\,. \tag{10}$$

The diffractive cross-section is given by the difference between the total and the sum over all cut cross-sections:

$$\frac{d\sigma_{diff}}{d^2b} = \frac{d\sigma_{tot}}{d^2b} - \sum_{k=1}^{\infty}\frac{d\sigma_k}{d^2b} = 2\left(1-\exp\left(-\frac{\Omega}{2}\right)\right) - (1-\exp(-\Omega)) = \left(1-\exp\left(-\frac{\Omega}{2}\right)\right)^2\,. \tag{11}$$

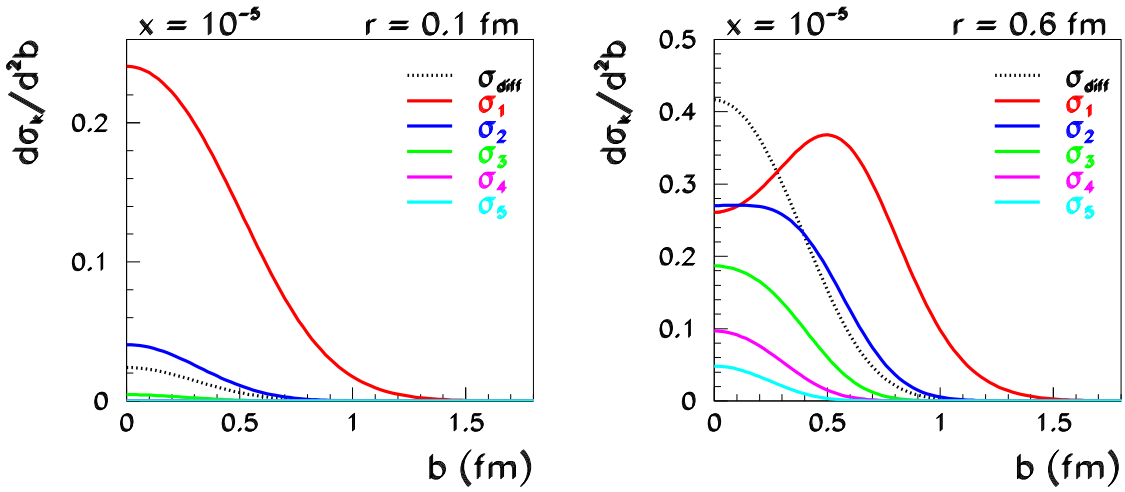

Fig. 8: Examples of b dependence of various cut dipole and diffractive cross-sections.

The cut cross-sections determined in the dipole model analysis of HERA data have several interesting properties shown in Fig. 8: for small dipoles ($r = 0.1$ fm) the opacity Ω is also small, so the single cut cross-section, σ_1, dominates. This leads to particle production emerging only from the one-cut pomeron, which should correspond, in the context of e.g. the LUND model, to a fragmentation of only one string. For larger dipoles ($r = 0.6$ fm) the dipole cross-section starts to be damped in the middle of the proton (at $b \approx 0$) by saturation effects. Therefore, the single cut cross-section is suppressed in the middle while the multiple cut cross-sections, σ_2, σ_3, etc, become substantial and increasingly concentrated in the proton center. These, fairly straight-forward properties of dipoles indicate that in the central scattering events the multiple scattering probability will be enhanced, which may lead at the LHC to substantial effects in a surrounding event multiplicity.

The contribution to F_2 from the k-cut Pomeron exchanges are computed in the analogous way to F_2:

$$F_2^k = \frac{Q^2}{4\pi^2\alpha_{em}}\int d^2r\int\frac{dz}{4\pi}\psi^*\psi\int d^2b\frac{d\sigma_k}{d^2b}. \tag{12}$$

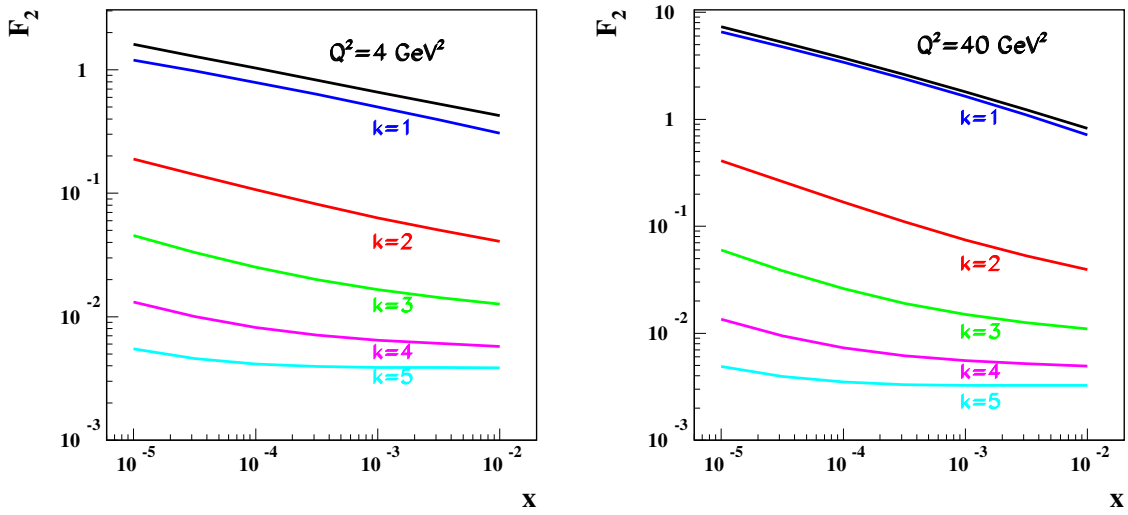

Fig. 9: F_2 and the contributions of k-cut Pomeron processes, F_2^k.

These contributions are shown, together with F_2, as a function of x for two representative Q^2 values in Fig. 9. One finds that multiple interaction contributions, i.e. $k \geq 2$, in the perturbative region, at $Q^2 = 4$ GeV^2, are substantial. In the typical HERA range of $x \approx 10^{-3} - 10^{-4}$, the $k = 2$ contribution is around 10% of F_2 and the contributions of higher cuts are also non-negligible. For example, the contribution of the 5-cut Pomeron exchanges is still around 0.5%, which means that at HERA, many thousand events may come from this type of process. Figure 10 shows the fraction of the multpile interaction processes,

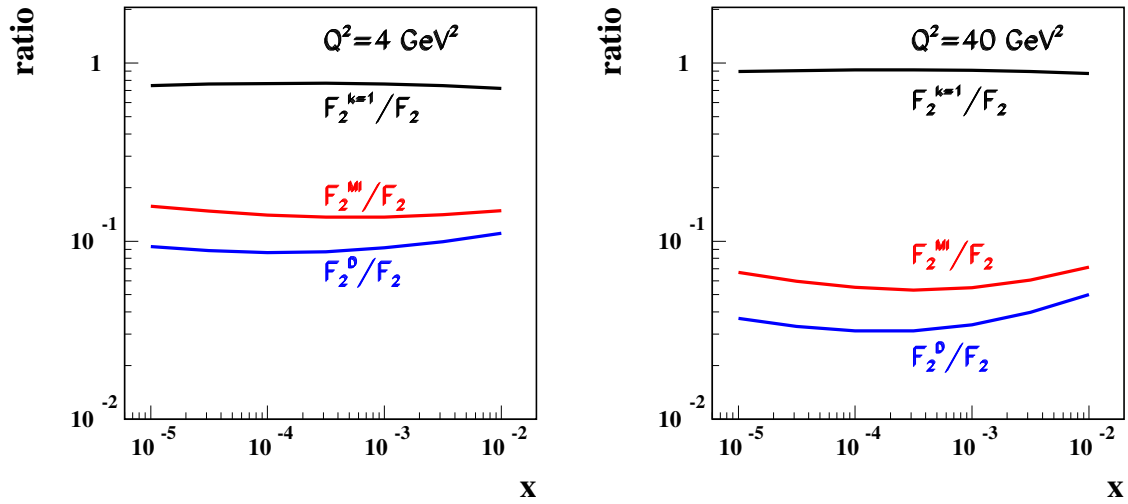

Fig. 10: Fractions of single (k=1), multiple interaction (MI) and diffraction (D) in DIS

$F_2^{MI} = F_2^{k=2} + F_2^{k=3} + F_2^{k=4} + F_2^{k=5}$ in F_2, at the same Q^2 values. At $Q^2 = 4$ GeV^2 the fraction of multiple scattering events is around 14% and at $Q^2 = 40$ GeV^2 around 6%, in the HERA x region, which indicates that the decrease of multiple scattering with increasing Q^2 is only logarithmic. The fraction of diffractive processes, shown for comparison, is of the same order, and drops also logarithmically with Q^2. The logarithmic drop of the diffractive contribution expected in the dipole model is confirmed by the data [6].

The dipole model provides a straight-forward extrapolation to the region of low Q^2, which is partly perturbative and partly non-perturbative. Figure 11 shows the contribution to F_2 of k-cut Pomeron processes and the fractions of multiple interactions and diffractive processes at $Q^2 = 0.4$ GeV^2.

Note also that, as a byproduct of this investigation, the ratio of diffractive and inclusive cross-sections, F_2^D/F_2 is found to be almost independent of x, in agreement with the data and also other dipole model predictions [6, 13, 14]. The absolute amount of diffractive effects is underestimated, since the evaluation of diffraction through AGK rules is oversimplified. It is well known [14], that a proper evaluation of diffraction should also take into account the $q\bar{q}g$ contribution which is missing in the simple AGK schema.

In conclusion, we find that the impact parameter dependent dipole saturation model [3] reproduces well the main properties of the data and leads to the prediction that multiple interaction effects at HERA should be of the order of diffractive effects, which are known to be substantial. The multiple interaction effects should decrease slowly (logarithmically) with increasing Q^2, similarly to the diffractive contribution.

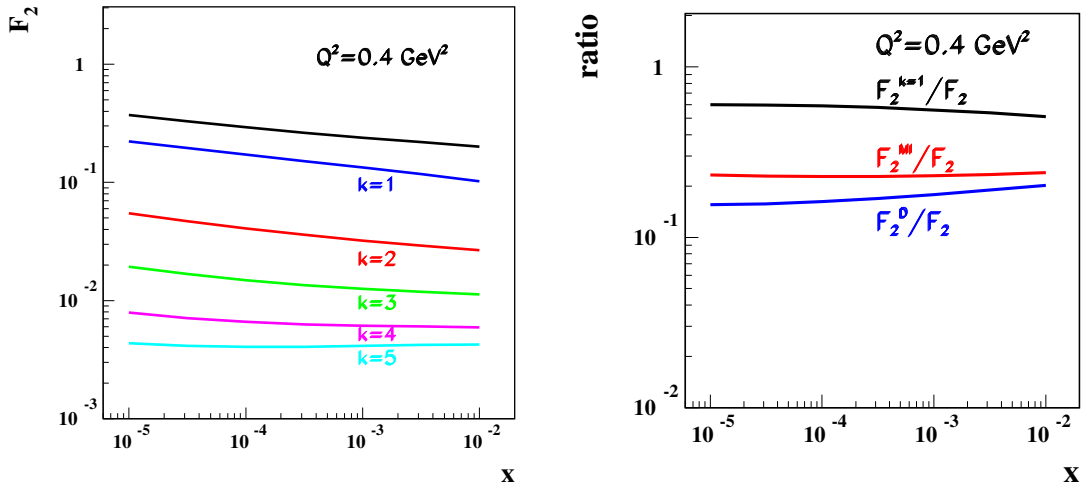

Fig. 11: Left: F_2 and the contributions of k-cut Pomeron processes. Right: Fractions of single (k=1), multiple interaction (MI) and diffraction (D) in DIS at $Q^2 = 0.4$ GeV^2.

4 Acknowledgements

I would like to thank Jochen Bartels for many illuminating discussions about physics of the multi-ladder QCD diagrams.

References

[1] G. Wolf, International Europhysics Conference on HEP (2001).
[2] Abramovski, Gribov, Kancheli, Sov. J. Nucl. Phys. **18**, 308 (1974).
[3] H. Kowalski and D. Teaney, Phys. Rev. D **68**, 114005 (2003).
[4] ZEUS Collaboration, S. Chekanov et al., Nucl. Phys. B **672**, 3 (2003).
[5] ZEUS Collaboration, S. Chekanov et al., Phys. Letters B **545**, 244 (2002).
[6] ZEUS Collaboration, S. Chekanov et al., Nucl. Phys. B **713**, 3 (2005).
[7] A. Levy, Nucl. Phys. B (Proc. Suppl) **146**, 92 (2005).
[8] J. Bartels and M. Ryskin, Z. Phys. **C 76**, 241 (1997).
[9] J. Bartels, M. Salvadore, and G.P. Vacca, Eur. Phys. J. C **42**, 53 (2005).
[10] N.N. Nikolaev and B.G. Zakharov, Z. Phys. C **49**, 607 (1991).
[11] A.H. Mueller, Nucl. Phys. B **415**, 373 (1994).
[12] A.H. Mueller and G.P. Salam, Nucl. Phys. B **475**, 293 (1996).
[13] K. Golec-Biernat and M. Wuesthoff, Phys. Rev. D **60**, 014023 (1999).
[14] J. Bartels, K. Golec-Biernat and H. Kowalski, Phys. Rev. D **66**, 014001 (2002).